Available online at www.sciencedirect.com
ScienceDirect
Journal of Power Sources 158 (2006) 1379–1385
JOURNAL OF POWER SOURCES
www.elsevier.com/locate/jpowsour

Structural characterization and electrochemical properties of RF-sputtered nanocrystalline Co_3O_4 thin-film anode

C.L. Liao, Y.H. Lee, S.T. Chang, K.Z. Fung *

Department of Materials Science and Engineering, National Cheng Kung University, No. 1, Ta-Hsueh Road, Tainan 70101, Taiwan

Received 14 April 2005; received in revised form 10 October 2005; accepted 11 October 2005
Available online 15 November 2005

Abstract

Nanocrystalline Co_3O_4 thin-film anodes were deposited on Pt-coated silicon and 304 stainless steel by radio frequency (RF) magnetron sputtering. The as-deposited and annealed cobalt oxide thin films showed smooth and crack-free morphologies. Both the as-deposited and annealed films exhibited spinel Co_3O_4 phase with nanocrystalline structure. High-temperature annealing enhanced the crystallinity of RF-sputtered cobalt oxide films due to rearrangement of cobalt and oxygen atoms. Electrochemical characterization of RF-sputtered films was carried out by cyclic voltammetry and charge/discharge tests in the voltage range of 0.3–3.0 V. Cyclic voltammetry plots showed that the RF-sputtered Co_3O_4 thin films were electrochemically active. X-ray photoelectron spectrometer (XPS) showed that the fresh cobalt oxide films had two peaks of Co_3O_4. In addition to the binding energy of cobalt oxide, the XPS spectrum of discharged film presented two additional binding energies correspond to Co metal. The first discharge capacities of as-deposited, 300, 500, and 700 °C-annealed films were 722.8, 772.5, 868.4, and 1059.9 $\mu Ah\,cm^{-2}\,\mu m^{-1}$, respectively. High-temperature annealing could enhance the capacity and cycle retention obviously. After 25 cycles discharging, the annealed films showed better cycle retention than as-deposited film. The 700 °C-annealed film exhibited excellent discharge capacity approximated to the theoretical capacity.

Keywords: Co_3O_4; RF-sputtering; Anode material; Lithium-ion battery

1. Introduction

Lithium-ion batteries have been extensively applied in several electric devices and portable electronics recently. Although carbon in nowadays is used as the commercial anode material due to its high specific capacity and good cycleability, it is still lay much stress on investigating new anode materials for rechargeable lithium-ion batteries. Recently, Poizot et al. [1,2] have reported nano-sized transition-metal oxides as new emerging anode materials due to their higher capacity compared to carbon anode. Thus, several metal oxides, such as FeO, CoO, NiO, Co_3O_4, SnO_2, Cu_2O, etc., were investigated as new anode materials for lithium-ion batteries [1–16]. The electrochemical mechanism of transition-metal oxides, is different from that of carbon material, is due to the oxidation of metal and reduction of metal oxide [1,2]. Li_2O decomposition and formation are going along with the redox reaction of metal oxides in addition. Among these metal oxide materials, Co_3O_4 has the highest specific capacity about 1100 $mAh\,g^{-1}$ when discharging to 0 V versus Li metal due to one Co_3O_4 can react with more than eight lithium ions. The overall reaction equation during charge/discharge is given as follows:

$$Co_3O_4 + 8Li \leftrightarrow 3Co + 4Li_2O$$

In addition to lithium-ion battery, thin-film microbattery is also a highly potential field to be researched. For lithium microbatteries, the electrochemical properties of thin-film electrodes prepared by various deposition methods were investigated. It can be prepared by pulse laser deposition (PLD) [14], electrochemical deposition (ECD) [17,18], sol–gel [19], and electron-beam evaporation [20] for application in lithium-ion batteries. However, articles about the electrochemical properties and structure characterization of RF-sputtered Co_3O_4 thin-film anode for lithium microbatteries were limited.

RF-sputtering is a simple and familiar technique for thin-film fabrication. In our previous works, we have used this method to

* Corresponding author. Tel.: +886 6 2380208; fax: +886 6 2380208.
E-mail address: kzfung@mail.ncku.edu.tw (K.Z. Fung).

0378-7753/$ – see front matter © 2005 Elsevier B.V. All rights reserved.
doi:10.1016/j.jpowsour.2005.10.014

obtain nanocrystalline lithium transition-metal oxide films as cathode materials [21,22]. In this study, Co_3O_4 thin-film anodes were deposited by RF-sputtering and the structure of the films was investigated by XRD and TEM analyses. Further, the electrochemical properties of RF-sputtered Co_3O_4 films were also conducted.

2. Experimental procedure

The cobalt oxide thin films were deposited by radio frequency magnetron sputtering (RF-sputtering) from a 2 in. diameter Co metal target in argon–oxygen (3:1) atmosphere with 12 standard cubic centimeter per minute (sccm) gas flow. The working pressure, RF power, and deposition time were 20 mTorr, 100 W, and 1 h, respectively. In order to increase the crystallinity of as-deposited cobalt oxide films, they have to undergo a post-annealing treatment in oxygen atmosphere. Pt-coated silicon ($Pt/Ti/SiO_2/Si$) and 304 stainless steel (thickness is 0.6 mm) were used as the substrates that were 40 mm away from the Co metal target. Even though the films deposited on various substrates showed similar morphologies, the adhesion of films deposited on stainless steels were better than on Pt-coated silicon.

Structure characterization of cobalt oxide thin films was investigated by X-ray diffraction method with multipurpose X-ray thin-film diffractometer (Rigaku, D/MAX2500) using Cu Kα radiation (λ = 1.5418 Å) and transition electron microscope (JOEL, 2010). The cross-sectional and surface morphology of cobalt oxide thin films were observed by scanning electron microscope (Philips, XL-40FEG). Electrochemical measurements include cyclic voltammetry and charge/discharge tests were also conducted. Both of these tests are investigated on $Li//Co_3O_4$ cell using RF-sputtered Co_3O_4 films as cathode (the active area is 1 cm^2), lithium metal as anode, and 1 M LiPF6 in propylene carbonate as electrolyte. The cyclic voltammetry (CV) tests were carried out by EG&G, Potentiostat 263A system under various scan speed (0.1–1.0 mV s^{-1}) and charge/discharge characteristics were measured by Arbin SCTS under a current density of 10 μA cm^{-2}. The voltage range for these two tests was in the range of 3.0–0.3 V. X-ray photoelectron spectrometer (XPS) measurement was performed on a PHI Quantera SXM system with Al Kα (1486.6 eV) irradiation. The base pressure of the vacuum chamber was better than 9×10^{-8} Torr.

3. Results and discussion

3.1. Structure characterization

The possible composition of the RF-sputtered film may consist of Co_3O_4, CoO, or other cobalt oxides. In this study, the structure characterization of RF-sputtered cobalt oxide films was analyzed by XRD and TEM. Fig. 1 shows the X-ray diffraction patterns of as-deposited, 300, 500, and 700 °C-annealed cobalt oxide films. It can be observed that two broad diffraction peaks locate at 2θ positions about 36.26° and 44.19°. Those two broad diffraction peaks may correspond to the (3 1 1) and (4 0 0) reflections of spinel Co_3O_4. This result indicates the as-deposited

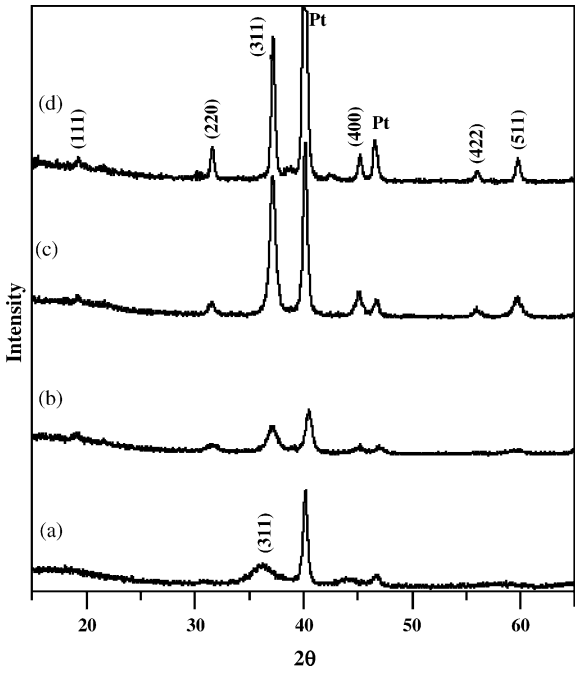

Fig. 1. XRD patterns of: (a) as-deposited, (b) 300 °C-annealed, (c) 500 °C-annealed, and (d) 700 °C-annealed cobalt oxide films.

Co_3O_4 film obtained by RF-sputtering may exhibit nanocrystalline structure. In addition, the (3 1 1) and (4 0 0) reflections are broad and observed to shift to lower 2θ position, indicating that the cobalt and oxygen atoms may not occupy their ideal lattice position of spinel structure completely. In other words, the shift of the broad reflections indicates that the as-deposited films are not well-crystallized spinel structure.

Fig. 1(b) shows the XRD pattern of 300 °C-annealed film, the intensity of (3 1 1) and (4 0 0) reflections slightly increase and shift to higher 2θ position (37.12° and 45.19°) compare to the as-deposited film. This result indicates the cobalt and oxygen atoms may occupy their ideal lattice position more completely, and consequently, the annealed film shows better crystallinity. After high-temperature annealing, the intensified Co_3O_4 reflections indicate that the annealed films exhibit polycrystalline spinel-structured Co_3O_4 with *Fd3m* space group. No cobalt metal or other cobalt oxides are observed in the XRD patterns, it indicates the RF-sputtered cobalt oxide films only consist of spinel Co_3O_4 phase. As shown in Fig. 1(b–d), all reflections of Co_3O_4 films finally become sharper after annealing from 300 to 700 °C. These results indicate that post-annealing process could enhance the crystallinity and enlarge the grain size of Co_3O_4 films. Furthermore, according to Scherrer equation [23], the grain sizes may be estimated from the width of the XRD peaks. It can be estimated that the grain size of as-deposited Co_3O_4 film is about 4 nm. Moreover, the grain sizes of annealed Co_3O_4 films were enlarged by the increasing annealing temperature due to grain growth of the films in high temperature. The grain sizes for 300, 500, and 700 °C-annealed Co_3O_4 films are approximated to be 7, 13, and 21 nm, respectively. These nano-sized grains were thought to exhibit better electrochemical activity than normal crystalline cobalt oxide anodes [12].

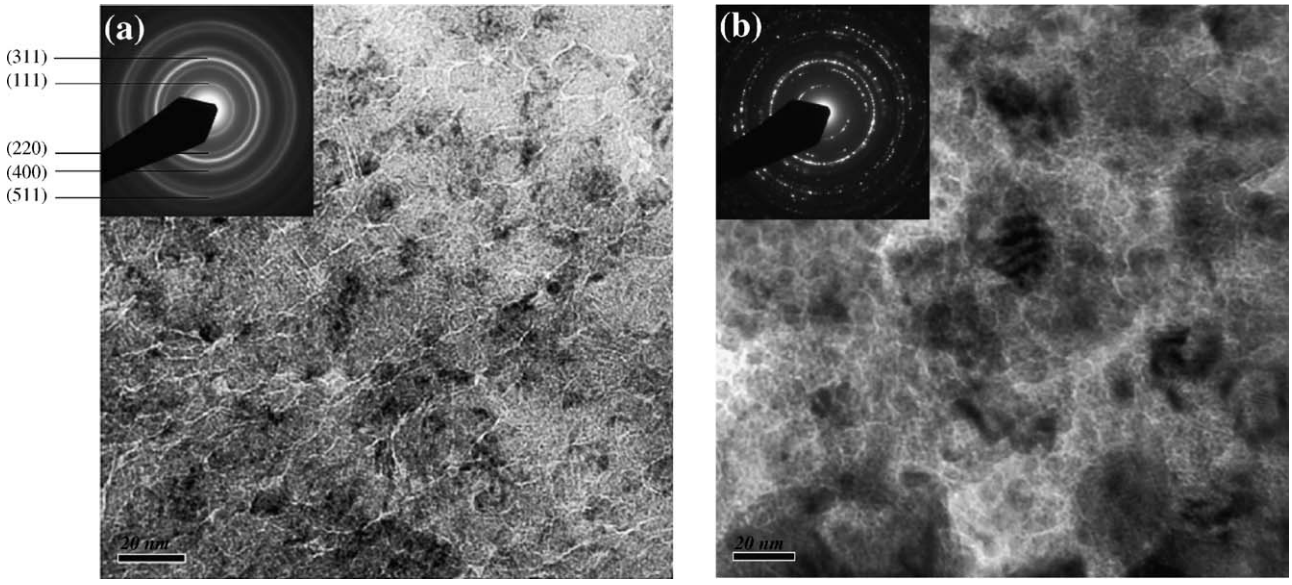

Fig. 2. TEM bright field images and selected area electron diffraction (SAED) patterns of: (a) as-deposited and (b) 700 °C-annealed cobalt oxide films.

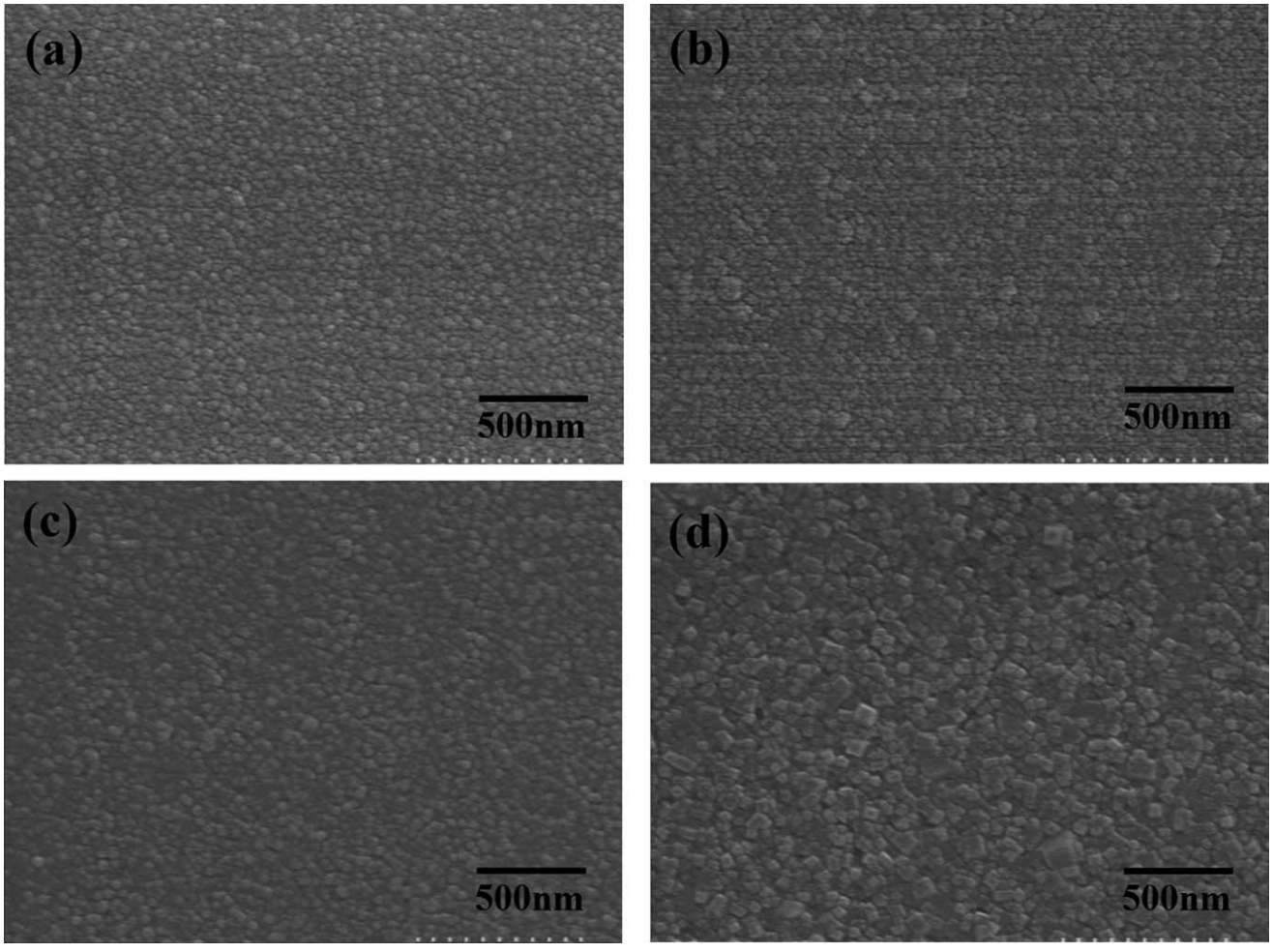

Fig. 3. SEM top-view micrographs of: (a) as-deposited, (b) 300 °C-annealed, (c) 500 °C-annealed, and (d) 700 °C-annealed cobalt oxide films; cross-sectional micrographs of: (e) as-deposited, (f) 300 °C-annealed, (g) 500 °C-annealed, and (h) 700 °C-annealed films.

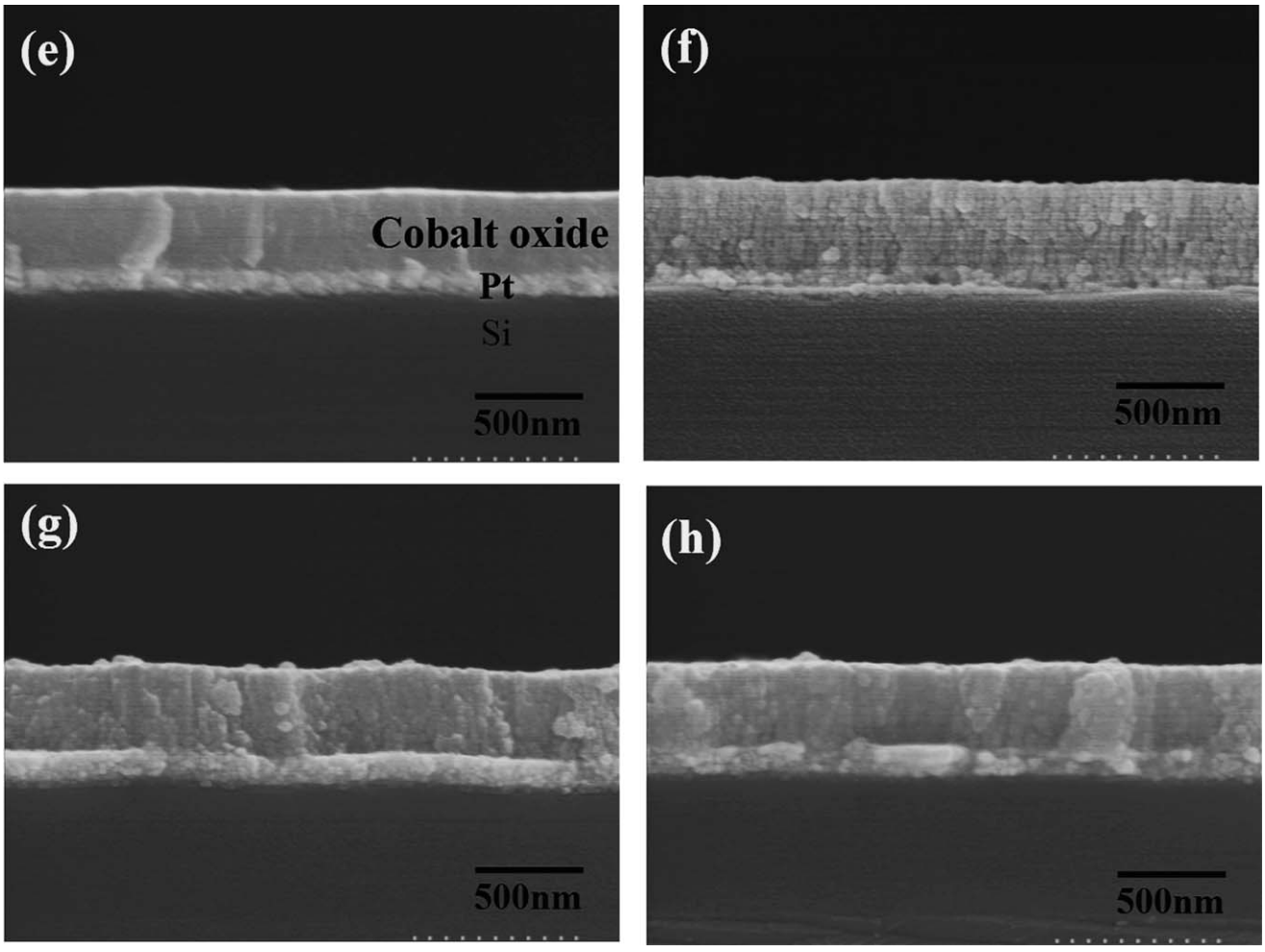

Fig. 3. (*Continued*).

It is well known that sufficient diffraction peaks is prerequisite in structure characterization by XRD. Nevertheless, in this study, the XRD reflections were insufficient to characterize the structure of as-deposited film. Therefore, TEM analysis is an additional evidence to confirm the structure of as-deposited films. Fig. 2(a) shows the TEM bright field image and selected area electron diffraction (SAED) pattern of as-deposited films. The SAED pattern is a typical diffraction pattern of spinel Co_3O_4 consist of broad (1 1 1), (2 2 0), (3 1 1), (4 0 0), (4 2 2), and (5 1 1) reflections. The broad rings in the SAED pattern indicate that the as-deposited cobalt oxide film consists of nanocrystalline structure. Fig. 2(b) shows the TEM bright field image and SAED pattern of 700 °C-annealed films. The SAED pattern shows that 700 °C-annealed film also consists of spinel Co_3O_4. Moreover, it indicates that the crystallinity was enhanced by high-temperature annealing. From TEM bright field images, it can be observed that as-deposited Co_3O_4 film consists of fine grains with the grain size less than 5 nm. Furthermore, the grain size was enlarged to about 25 nm after 700 °C-annealing. The grain sizes observed from TEM analysis are in the same order of magnitude as that estimated from XRD patterns.

3.2. SEM observation

Fig. 3(a–d) shows the SEM micrographs of RF-sputtered Co_3O_4 films deposited on Pt-coated silicon viewing from the top under various annealing conditions. The surface morphologies of as-deposited and annealed Co_3O_4 films are all smooth and crack-free. Nanocrystalline grains are observed from all the top-view micrographs. It is obviously that grain sizes increase with the increasing annealing temperature due to grain growth in the annealing process, thus, square grains are observed after 700 °C-annealing process. Fig. 3(e–h) shows the cross-sectional images of as-deposited and annealed cobalt oxide films. From the cross-sectional observations, the films show columnar structure that was commonly observed in RF-sputtered films. Moreover, the thicknesses of as-deposited and annealed films were all about 370 nm. After several cycles of charge/discharge test, the adhesion of films on stainless steel was better than on Pt-coated silicon even though the morphologies and thicknesses of cobalt oxide films on both substrates were exceedingly similar. Consequently, films deposited on stainless steel were used in the following electrochemical characterizations due to the better adhesion between film and substrate.

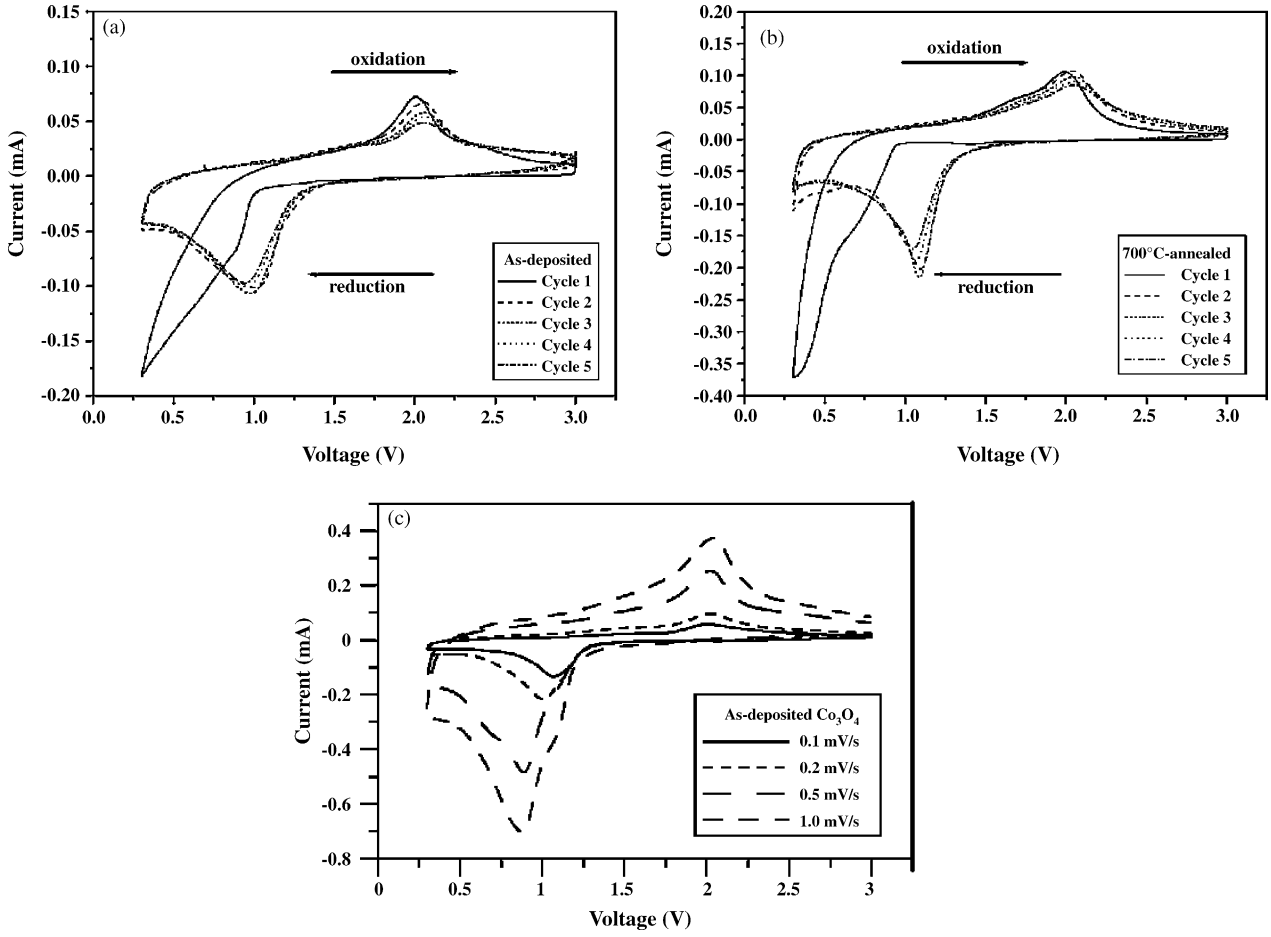

Fig. 4. Cyclic voltammetry (CV) plots of: (a) as-deposited, (b) 700 °C-annealed Co_3O_4 films conducted under scan rate of 0.1 mV s^{-1}, and (c) as-deposited film that was measured under various scan rates.

3.3. Electrochemical characterization

Electrode materials of lithium batteries usually exhibit electrochemical activity to react with lithium ions. In order to distinguish the electrochemical activity of material, cyclic voltammetry (CV) analysis is an authoritative method to be utilized. Fig. 4(a and b) shows the CV plots of as-deposited and 700 °C-annealed cobalt oxide films, respectively. One set of redox peaks, including a reduction peak at about 1 V and an oxidation peak at about 2 V, are observed in all CV plots. These results indicate that there was only one reaction in the reduction/oxidation process. Moreover, the integrated area of redox peaks also implies some information. (I) The integrated areas of redox peaks of as-deposited film are smaller than that of annealed film. It indicates that the capacity of annealed films might be better than that of as-deposited films. (II) The integrated area of redox peaks decreases noticeably along the increasing cycle number in as-deposited films. Nevertheless, the integrated area of redox peaks of 700 °C-annealed films only shows slightly variation. Consequently, the CV results indicate that annealed films with better crystallinity might exhibit better electrochemical properties (capacity and cycle retention) than that of as-deposited films. Furthermore, it is conjectured that the capability of RF-sputtered cobalt oxide film is highly related to its crystallinity. Additionally, CV plots with various scan rates were also conducted as shown in Fig. 4(c). It can be observed that the peak separation was enlarged with the increasing scan rate. It may be possible to obtain the average diffusion coefficient $\tilde{D}$ of Li^+ in cobalt oxide films by the following equation [24]:

$$i_p = 0.4463nFAC\tilde{D}^{1/2}\left(\frac{nF}{RT}\right)^{1/2}v^{1/2}$$

Based on this equation, the Li^+ diffusion coefficient $\tilde{D}$ was estimated in the range of $(1.4–5.2) \times 10^{-12}$ cm^2 s^{-1}.

The electrochemical mechanism of transition-metal oxide anodes was extensively investigated recently. In this study, XPS was used to examine the changes of the specimens before and after discharge step. Fig. 5(a) shows the XPS spectrum of 700 °C-annealed Co_3O_4 film before discharge. In Fig. 5(a), it can be observed that two peaks locate at binding energy of 780.6 and 795.6 eV correspond to Co $2p_{3/2}$ and Co $2p_{1/2}$ of Co_3O_4, respectively. Even though the cobalt oxides, CoO and Co_3O_4, might show similar XPS spectra. According to the XRD results showed previously, the XPS spectrum of 700 °C-annealed film is believed to be spinel Co_3O_4. Moreover, the Co $2p_{3/2}$–Co $2p_{1/2}$ splitting of approximately 15 eV in Fig. 5(a) is associated with spinel Co_3O_4 [25–27]. In addition, the XPS spectrum of 700 °C-

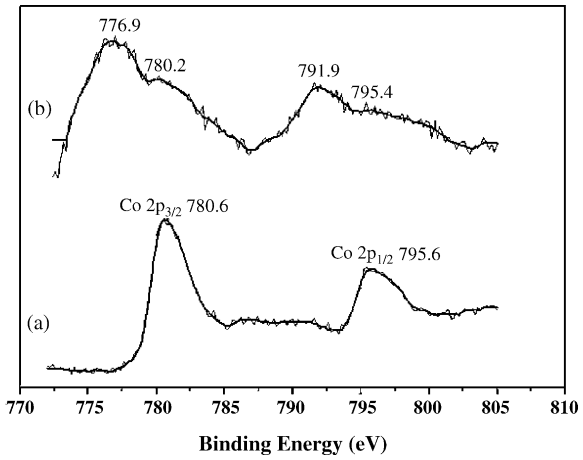

Fig. 5. XPS spectra of 700 °C-annealed Co_3O_4 films that were: (a) before and (b) after discharging to 0.3 V.

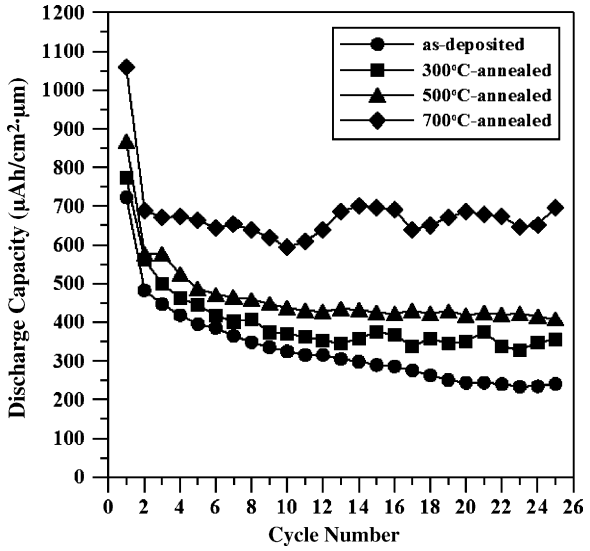

Fig. 6. Discharge capacity vs. cycle number plots of as-deposited and annealed films.

annealed film that was discharged to 0.3 V is shown in Fig. 5(b). In addition to the two binding energies of Co_3O_4, there are two additional binding energies (776.9 and 791.9 eV) correspond to Co $2p_{3/2}$ and Co $2p_{1/2}$ of Co metal. The formation of Co from Co_3O_4 after discharging is thermodynamically feasible and can be expected. Poizot et al. have conducted a study on the electrochemical properties of several transition-metal oxides for Li-ion batteries [1,2]. The electrochemical reactions are shown as follows:

$$\text{Cathode}: \quad Co_3O_4 + 8Li^+ + 8e^- \leftrightarrow 3Co + 4Li_2O \tag{1}$$

$$\text{Anode}: \quad 8Li \leftrightarrow 8Li^+ + 8e^- \tag{2}$$

$$\text{Overall reaction}: \quad Co_3O_4 + 8Li \leftrightarrow 3Co + 4Li_2O \tag{3}$$

In general, Li_2O was always reported to be electrochemically inactive. However, many recent articles demonstrated the electrochemical reversibility of Li_2O by TEM or XPS [1,10,11,15,28,29]. They described that the nano-sized transition-metal particles and Li_2O formed during discharge process, and then, those nano-sized transition-metal particles could decompose Li_2O in the following charge step. It was believed that nano-sized metal particles with large free surface area could activate the nanocrystalline Li_2O and promote its electrochemical reversibility. Therefore, based on those articles [15,28] and the XPS results in this study, it is believed that Co nano-particles formed from Co_3O_4 nano-particles in discharge step, and, afterward the Co nano-particles can further activate the decomposition of Li_2O during the charge process.

The discharge capacity of as-deposited and annealed Co_3O_4 films plots as a function of cycle number is shown in Fig. 6. The first discharge capacity of as-deposited film is 722.8 $\mu Ah\,cm^{-2}\,\mu m^{-1}$. Moreover, after the sputtered film underwent annealing process, the first discharge capacity increased to 772.5, 868.4, and 1059.9 $\mu Ah\,cm^{-2}\,\mu m^{-1}$ for 300, 500, and 700 °C-annealed films, respectively. These results indicate that discharge capacity is extremely relate to the annealing temperature as a result of the enhancement of crystallinity of sputtered Co_3O_4 films. It was suggested that the well-crystalline Co_3O_4 may exhibit better electrochemical activity result in formation of Co nano-particles completely and uniformly. Thus, the complete and uniform formation of Co nano-particles can effectively activate the decomposition of Li_2O. It can be also observed that the second discharge capacity showed a large fading compared to the first discharge, which was usually observed in transition-metal oxide anodes. After the second discharge, the discharge capacity only shows slight decay in the following discharge test. Moreover, annealed films also exhibit better cycle retention than as-deposited film. After 25 cycles discharging, the 25th discharge capacities for as-deposited, 300, 500, and 700 °C-annealed films are 240.8, 354.6, 408.5, and 695.1, respectively. Basically, Co_3O_4 exhibits theoretical capacity that is estimated about 700 $\mu Ah\,cm^{-2}\,\mu m^{-1}$. Therefore, the 700 °C-annealed cobalt oxide films still shows excellent capability even after 25 cycles test. It indicates that RF-sputtered nanocrystalline Co_3O_4 films exhibit well electrochemical properties to be applied as a new anode material in energy storage application.

4. Conclusion

Smooth and crack-free RF-sputtered Co_3O_4 thin films were characterized as electrochemically active material for lithium batteries. The as-deposited and annealed films exhibited spinel Co_3O_4 single phase with nanocrystalline structure. From XRD estimations, the grain size for Co_3O_4 films were about 4–25 nm. Moreover, the formation of Co metal after discharging step was demonstrated by XPS analysis. Consequently, the electrochemical reversibility of Co_3O_4 thin films can be attributed to the reversible reactions of Co_3O_4 to Co metal and Li to Li_2O. Discharge capacity and cycle retention can be enhanced by annealing due to the increased crystallinity of the films. In this study, RF-sputtered Co_3O_4 thin films showed excellent electrochemical properties, especially the 700 °C-annealed films exhibited discharge capacity that approximated to the theoretical capacity.

Acknowledgement

This work is financially supported by the National Science Council of Taiwan, ROC (Grant No. NSC 94-2120-M-006-002).

References

[1] P. Poizot, S. Laruelle, S. Grugeon, L. Dupont, J.-M. Tarascon, Nature 407 (2000) 496.
[2] P. Poizot, S. Laruelle, S. Grugeon, L. Dupont, J.-M. Tarascon, J. Power Sources 97–98 (2001) 235.
[3] D. Larcher, G. Sudant, J.-B. Leriche, Y. Chabre, J.-M. Tarascon, J. Electrochem. Soc. 149 (2002) A234.
[4] G.X. Wang, Y. Chen, K. Konstantinov, M. Lindsay, H.K. Liu, S.X. Dou, J. Power Sources 109 (2002) 142.
[5] Z.Y. Yuan, F. Huang, C.Q. Feng, J.T. Sun, Y.H. Zhou, Mater. Chem. Phys. 79 (2003) 1.
[6] S. Laruelle, S. Grugeon, P. Poizot, M. Dolle, L. Dupont, J.-M. Tarascon, J. Electrochem. Soc. 149 (2002) A627.
[7] P. Poizot, S. Laruelle, S. Grugeon, J.-M. Tarascon, J. Electrochem. Soc. 149 (2002) A1212.
[8] D. Larcher, C. Masquelier, D. Bonnin, Y. Chabre, V. Masson, J.-B. Leriche, J.-M. Tarascon, J. Electrochem. Soc. 150 (2003) A133.
[9] D. Larcher, D. Bonnin, R. Cortes, I. Rivals, L. Personnaz, J.-M. Tarascon, J. Electrochem. Soc. 150 (2003) A1643.
[10] A. Debart, L. Dupont, P. Poizot, J.-B. Leriche, J.-M. Tarascon, J. Electrochem. Soc. 148 (2001) A1266.
[11] S. Grugeon, S. Laruelle, R. Herrera-Urbina, L. Dupont, P. Poizot, J.-M. Tarascon, J. Electrochem. Soc. 148 (2001) A285.
[12] G.X. Wang, Y. Chen, K. Konstantinov, J. Yao, J.-H. Ahn, H.K. Liu, S.X. Dou, J. Alloys Compd. 340 (2002) L5.
[13] S.T. Chang, I.C. Leu, C.L. Liao, J.H. Yen, M.H. Hon, J. Mater. Chem. 14 (2004) 1821.
[14] Y. Wang, Z.-W. Fu, Q.-Z. Qin, Thin Solid Films 441 (2003) 19.
[15] V. Pralong, J.-B. Leriche, B. Beaudoin, E. Naudin, M. Morcrette, J.-M. Tarascon, Solid State Ionics 166 (2004) 295.
[16] R. Yang, Z. Wang, J. Liu, L. Chen, Electrochem. Solid-State Lett. 7 (2004) A496.
[17] K. Nakaoka, M. Nakayama, K. Ogura, J. Electrochem. Soc. 149 (2002) C159.
[18] C.N.P. da Fonseca, M.-A. de Paoli, A. Gorenstein, Adv. Mater. 3 (1991) 553.
[19] F. Svegl, B. Orel, I.G. Svegl, V. Kaucic, Electrochim. Acta 45 (2000) 4359.
[20] T. Seike, J. Nagai, Sol. Energy Mater. 22 (1991) 107.
[21] C.L. Liao, K.Z. Fung, J. Power Sources 128 (2004) 263.
[22] C.L. Liao, Y.H. Lee, H.C. Yu, K.Z. Fung, Electrochim. Acta 50 (2004) 459.
[23] B.D. Cullity, Elements of X-Ray Diffraction, Addison Wesley, 1977.
[24] A.J. Bard, L.R. Faulkner, Electrochemical Methods, second ed., Wiley, New York, 2001, p. 231.
[25] N.S. Mclntyre, M.G. Cook, Anal. Chem. 47 (1975) 2208.
[26] C.V. Schenck, J.G. Dillard, J. Colloid Interface Sci. 95 (1983) 398.
[27] B. Ernst, S. Libs, P. Chaumette, K. Alain, Appl. Catal. A 186 (1999) 145.
[28] Y.-M. Kang, M.-S. Song, J.-H. Kim, H.-S. Kim, M.-S. Park, J.-Y. Lee, H.K. Liu, S.X. Dou, Electrochim. Acta 50 (2005) 3670.
[29] R. Dedryvère, S. Laruelle, S. Grugeon, P. Poizot, D. Gonbeau, J.-M. Tarascon, Chem. Mater. 16 (2004) 1056.